NORIAKI ISHII
Associate Professor,
Faculty of Technology,
Osaka Electro-Communication University,
Osaka, Japan
Assoc. Mem. ASME

KENSAKU IMAICHI
Professor.
Mem. ASME

AKIO HIROSE
Graduate Student.

Faculty of Engineering Science,
Osaka University,
Osaka, Japan

Instability of Elastically Suspended Tainter-Gate System Caused by Surface Waves on the Reservoir of a Dam

In this study, it is theoretically shown that an elastically suspended Tainter-gate system with damping effects possesses the property of a self-excited oscillation, provided that the center of the curved weir plate is not in agreement with the location of the trunnion pin. Moreover, the theoretically obtained characteristics for the self-excited oscillation are confirmed with experiments, and it is shown that the theoretical results are in good agreement with experiments. It is concluded that when designing a dam system with Tainter-gates or other similar devices, more interest and attention to the dynamical behavior of Tainter-gates should be taken in order to prevent disasters such as that which occurred in Japan.

Introduction

At present, Tainter-gates [2, 3][1] are being used with increased frequency in Japan, in order to control the water level of reservoirs. Vertical-lift gates also are being used for the same purpose. In this type, however, as the frame of the gate bears directly on the downstream guide member, a great frictional resistance occurs at the contact plane between the two. Therefore, a large hoist capacity is required not only for raising but for lowering as well. This fact limits its use to the smaller sizes. In the type of Tainter-gates, on the contrary, as the resultant of the hydraulic pressure exerted on the weir plate generally passes near the trunnion pin and is nearly borne at the trunnion pin as shown in Fig. 1, the effect of mechanical frictions in the Tainter-gate system is much less than in the type of vertical-lift gates, therefore providing a small hoisting load and a smooth operation of the gate. Hence the Tainter-gate is suited for the larger sizes. Though Tainter-gates have such advantages, there is concern that Tainter-gates may oscillate owing to some fluid-induced structural load, i.e. the operation of the Tainter-gates may tend to become unstable.

In Japan, several years ago, a Tainter-gate collapsed while the gate was being opened to discharge water [4]. This accident caused a sudden rise in the water level of the lower reaches of a stream and took a toll of human lives. Although the collapse of the Tainter-gate occurred by the buckling of the stays, very careful consideration had been given to the static strength of the structure in designing. Therefore it has been considered that the buckling of the stays was caused by some fluid-induced dynamical load. Many studies have been made for Tainter-gates under a steady discharge [5–7]. Little, however, has been known about the dynamical characteristics of Tainter-gates.

One of the subjects for the dynamic behavior of Tainter-gates is that they may essentially possess the property of a self-excited oscillation. Tainter-gates are usually suspended with chains or cables attached near the bottom of the weir plate. Such chains or cables act as an elastic support. Therefore an oscillatory system interfering with fluid-induced loads is formed. For example, when the weir plate is slightly displaced from its equilibrium position, a change of discharge rate is caused, wave motions are induced on the reservoir surface and the wave motions exert a transient hydrodynamical force on the weir plate. It is not always expected that the hydrodynamical force makes the oscillatory displacement of the weir plate decay, but may be dynamically increased by the hydrodynamical force since the damping effect in the mechanism is comparatively small. In such a case, a self-excited oscillatory system is formed. Careful considerations should be given to the possibility of such a self-excited oscillation in designing Tainter-gates.

The characteristics of surface waves and structural loads induced by a forced and periodical change of discharge quantity were theoretically analyzed, as the first approach for analyzing the dynamical characteristics of Tainter-gates [8]. It was concluded as follows: A basic parameter determining the characteristics of surface waves and structural loads is the Froude number $F'_0 = \sqrt{d_0/g} \cdot \omega$. The characteristics of surface waves are very analogous to the resonance characteristics of the forced oscillatory system consisting of a mass, a spring and a damper. When the Froude number is equal to about 0.8, wave motions fall into a resonance state. Moreover, the characteristics of fluid-induced structural loads suggested the possibility of a self-excited oscillation for Tainter-gates. These theroetical results were proved by experiments. The stability of an idealized

[1]Numbers in brackets designate References at end of paper.

Contributed by the Fluids Engineering Division of The American Society of Mechanical Engineers and presented at the Joint Applied Mechanics, Fluids Engineering & Bioengineering Conference, New Haven, Conn., June 15–17, 1977. Manuscript received at ASME Headquarters March 25, 1977. Paper No. 77-FE-25.

Tainter-gate system without damping effects was theoretically analyzed, as the second approach, but the analysis was restricted to the case that the resultant of the hydraulic pressure exerted on the weir plate passes under the trunnion pin [9]. It was concluded as follows: Tainter-gates fundamentally possess the property of a self-excited oscillation.

In this study, the stability of an actual Tainter-gate system with damping effect is theoretically analyzed, for the general case that the resultant of the hydraulic pressure exerted on the weir plate does not pass through the trunnion pin, but the analysis is restricted to the case that a steady discharge is comparatively small. It is concluded as follows: The Tainter-gate system grows up to a self-excited oscillatory system under an appropriate condition, even if there exist comparatively large damping effects in the system. A model experiment for Tainter-gates is made in order to confirm the theoretical results. It is concluded that the Tainter-gate system actually grows up to a self-excited oscillatory system, and the theoretically obtained results for the self-excited oscillation are in good agreement with the experiments.

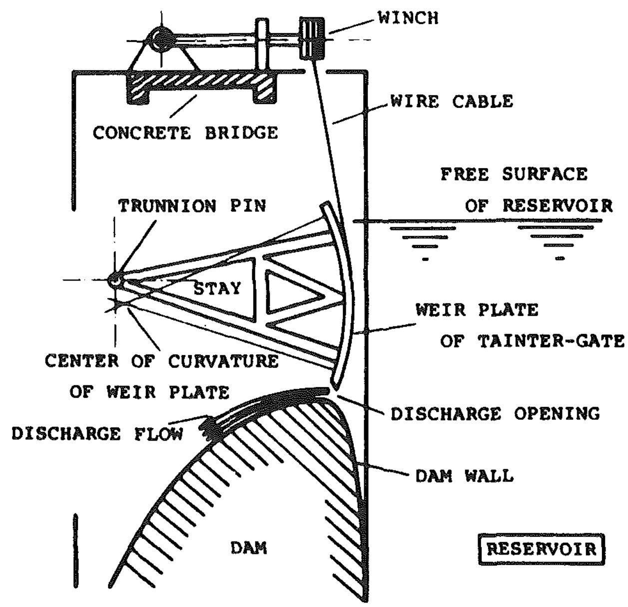

Fig. 1 A Tainter-gate system

The Transient Hydrodynamical Pressure Exerted on the Weir Plate and the Equation of Motion of the Tainter-Gate System

The Tainter-gate system shown in Fig. 1 is assumed to be represented by the two-dimensional model shown in Fig. 2. The Tainter-gate OAB is elastically suspended from a concrete bridge and is able to rotate on the trunnion pin 0. When the equilibrium state shown in Fig. 2 is kept, the moment about the trunnion pin 0 due to the weight of the Tainter-gate itself and the hydraulic pressure exerted on the weir plate is equal to that due to the restoring force of an elastic support. In this paper, the dynamical stability of such an equilibrium state of the Tainter-gate system is analyzed. In this section, the equation of motion to which the small oscillation of the Tainter-gate from the equilibrium state is subject, is derived.

To analyze the oscillation of the Tainter-gate, the X, Y, Z-coordinate system with the X-axis taken horizontally, the Y-axis vertically upward and the Z-axis in the rotatory axis of the Tainter-gate is used. $\theta(t)$ denotes the small rotatory angle from the equilibrium state of the Tainter-gate about the Z-axis. $\theta(t)$ is defined as positive when the Tainter-gate rotates in the direction of the arrow shown in Fig. 2. To analyze the transient hydrodynamical pressure exerted on the weir plate, the x, y-coordinate system with the y-axis taken vertically upward through the point B and the x-axis in the original undisturbed horizontal free surface of the reservoir is used. To simplify the treatment of the problem, the distance between the vector of the hydrodynamical pressure exerted on the weir plate and the trunnion pin 0 is assumed to be approximately constant R_*. Furthermore, it is assumed that all of the damping effects in the Tainter-gate system, for example, due to the mass of the fluid added to the movement of the weir plate and the hydraulic or mechanical frictions arising at the pairs of elements in the mechanism, are represented by a viscous damper vertically attached to the point B, as shown in Fig. 2.

Nomenclature

a = small constant
A = arbitrary function
b = height of discharge
c_f = discharge coefficient
c_g = modification factor of area
d_0 = depth of discharge opening
F = Froude number, $\sqrt{d_0/g} \cdot \omega$
F_0 = general Froude number
F'_0 = basic Froude number
g = gravity acceleration
G = coefficient function
i = imaginary unit, $\sqrt{-1}$
I_0 = moment of inertia
k' = design factor
K_0 = spring constant
m, s = variables of Fourier cosine transform
M = moment
p = transient hydrodynamical pressure
p' = complex variable, $\xi'_p + i\eta'_p$
q = amplitude of $\Delta Q(t)$
R_a, R_b = length of stays
R'_d = dimensionless depth
R_* = eccentric radius of trunnion pin
s' = $d_0 s$
s'_0 = complex variable
u' = real part of $w'(p')$
u'_* = Nyquist characteristic function
v' = imaginary part of $w'(p')$
v'_* = Nyquist characteristic function
w' = dimensionless characteristic function
x = coordinate along undisturbed reservoir surface
x' = x/d_0
y = coordinate normal to undisturbed reservoir surface
y' = y/d_0
X = coordinate along the horizontal direction
Y = coordinate taken vertically upward
Z = coordinate taken in trunnion pin
γ_0 = damping coefficient of viscous damper
Γ = contour
ΔQ = change of discharge quantity
ζ = damping ratio
η_p = general frequency
η'_p = imaginary part of p'
θ = small rotatory angle
$\dot{\theta}_0$ = initial angular velocity
Θ = angle between stays
μ, μ' = small positive constant
ξ'_p = real part of p'
ρ = density
τ = integration variable
ϕ = velocity potential
$\bar{\phi}$ = Fourier cosine transform of ϕ
$\bar{\phi}^{(p)}$ = particular solution
$\bar{\bar{\phi}}^{(p)}$ = Fourier cosine transform of $\bar{\phi}^{(p)}$
ϕ_0 = phase function
ω = frequency of fluctuating discharge
ω_0 = natural frequency

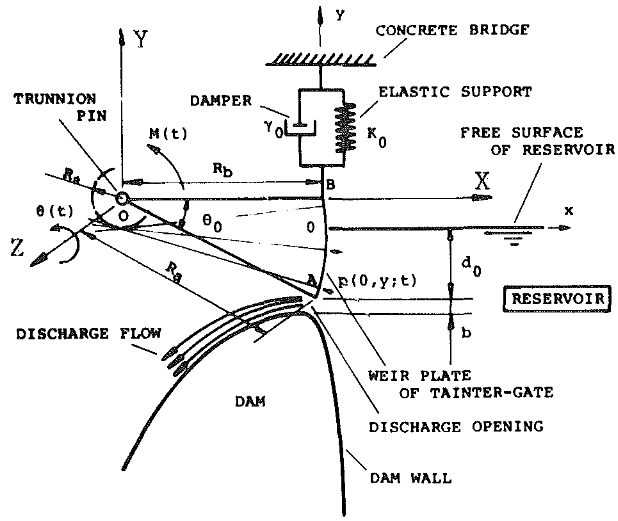

Fig. 2 A two-dimensional model for the Tainter-gate system

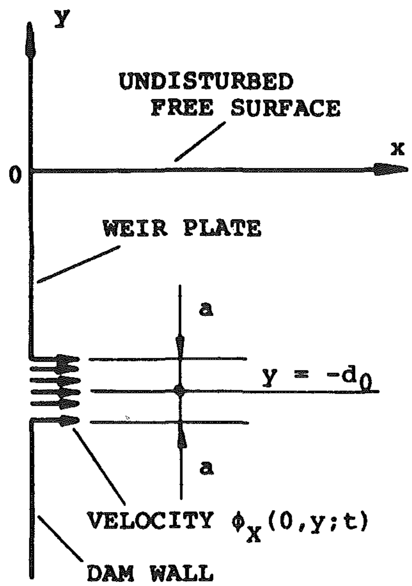

Fig. 3 A two-dimensional model for the flow in the reservoir

The Transient Hydrodynamical Pressure Exerted on the Weir Plate. It is assumed that the fluid in the reservoir is incompressible, the flow in the reservoir two-dimensional, the depth of the reservoir infinite and there are no obstacles obstructing the progress of surface waves at the upper reaches of the reservoir. Furthermore, the subject is restricted to the case that the height b of the discharge opening is very small compared with the depth d_0 of the discharge opening. When this condition is satisfied, the effect of a steady discharge is entirely negligible in deriving the transient hydrodynamical pressure exerted on the weir plate.

When some disturbance is given to the Tainter-gate under a steady discharge and the Tainter-gate rotates by a small angle $\theta(t)$ from the equilibrium state, the change $\Delta Q(t)$ of the discharge quantity from the discharge opening is given by the following form:

$$\Delta Q(t) = q \cdot \theta(t), \tag{1}$$

where, since the natural frequency of the Tainter-gate system is comparatively small, it may be assumed that there is no delay of phase between the movement of the weir plate and the change of discharge quantity. Since the rotatory motion of the Tainter-gate has been assumed to be comparatively small, the amplitude q of the fluctuating discharge quantity $\Delta Q(t)$ may be given by

$$q = c_f\sqrt{2dg_0} \cdot R_a \cos \Theta_0, \tag{2}$$

where c_f is a discharge coefficient for the Tainter-gate. The velocity potential $\phi(x, y; t)$ must be a solution of the Laplace equation:

$$\phi_{xx} + \phi_{yy} = 0. \tag{3}$$

Since the dam wall and the weir plate are generally curved as shown in Fig. 2, the equation (3) should be solved under such curved boundaries to be exact. To simplify the analysis of the subject, however, it is assumed that the dam wall and the weir plate can be replaced with the linear boundaries as shown in Fig. 3. Furthermore, it is assumed that the movement of the boundary in the neighborhood of the discharge opening can be neglected, and the change of the discharge quantity is concentrated at the point $(x, y) = (0, -d_0)$: one need only suppose that the height of discharge $2a \rightarrow 0$ while the discharge velocity $\phi_x(0, y; t) \rightarrow \infty$ in such a way that the total change of discharge quantity $-\int_{-d0-a}^{-d_0+a} \phi_x(0, y; t)dy$ tends to the finite limit $\Delta Q(t)$ from (1):

$$\Delta Q(t) = -\lim_{a\rightarrow 0} \int_{-d0-a}^{-d_0+a} \phi_x(0, y; t)dy. \tag{4}$$

To represent in a rough way the effect of small dissipative forces in the fluid, the damping force first given by J. W. S. Rayleigh [10, 11] and H. Lamb [12, 13] which is proportional to the velocity of the fluid particles is assumed. Then the boundary condition on the free surface is given by the following form:

$$[\phi_{tt} + \mu\phi_t + g\phi_y]_{y=0} = 0, \tag{5}$$

where the coefficient μ in the dissipative force is a small positive constant. Since the velocity potential $\phi(x, y; t)$ represents a small change from the equilibrium state, the small quantities of the second order have been neglected. The boundary conditions on the other boundaries except for the discharge opening and the free surface are given as follows:

$$\begin{aligned} \phi_x(0, y; t) = 0 \quad \text{when} \quad & -\infty < y < -d_0 + a, \\ & -d_0 + a < y \leqq 0 (a \rightarrow 0), \\ \phi_x(\infty, y; t) = 0,\ & \phi(\infty, y; t) = 0, \\ \phi_y(x, -\infty; t) = 0,\ & \phi(x, -\infty; t) = 0, \end{aligned} \tag{6}$$

where the boundedness conditions have been imposed on the boundaries at $x = \infty$ and at $y = -\infty$. At the time $t = 0$ the following initial conditions are prescribed for the velocity potential $\phi(x, y; t)$:

$$\phi(x, 0; 0) = 0, \quad \phi_t(x, 0; 0) = 0, \tag{7}$$

which state that the free surface is initially at rest in its horizontal equilibrium position. Furthermore, at the time $t = 0$ the following initial conditions are prescribed for the rotatory angle $\theta(t)$:

$$\theta(0) = 0, \quad \theta_t(0) = \dot{\theta}_0, \tag{8}$$

which state that the Tainter-gate suddenly begins to rotate with the angular velocity $\dot{\theta}_0$ from the equilibrium state.

To obtain a solution of the Laplace equation (3) satisfying the boundary conditions (4), (5), (6) and the initial conditions (7) and (8), the Fourier cosine transform in the variable x is applied to (3):

$$\bar{\phi}_{yy}(s, y; t) - s^2\bar{\phi}(s, y; t) = \sqrt{2/\pi}\phi_x(0, y; t), \tag{9}$$

in which $\bar{\phi}(s, y; t)$ is the Fourier cosine transform of $\phi(x, y; t)$

and use has been made of the boundary conditions at $x = \infty$ in (6). The solution of (9) is given by the following form:

$$\bar{\phi}(s, y; t) = \bar{\phi}^{(p)}(s, y; t) + A(s; t)e^{sy}. \quad (10)$$

The particular solution $\bar{\phi}^{(p)}(s, y; t)$ must satisfy the following boundary conditions corresponding to the conditions at $y = -\infty$ in (6):

$$\bar{\phi}_y^{(p)}(s, -\infty; t) = 0, \quad \bar{\phi}^{(p)}(s, -\infty; t) = 0. \quad (11)$$

The following boundary condition at $y = 0$ may be imposed for $\bar{\phi}^{(p)}(s, y; t)$:

$$\bar{\phi}_y^{(p)}(s, 0; t) = 0. \quad (12)$$

To obtain the particular solution $\bar{\phi}^{(p)}(s, y; t)$ the Fourier cosine transform in the variable y is applied to (9):

$$(m^2 + s^2)\tilde{\bar{\phi}}^{(p)}(s, m; t) = -(2/\pi)\int_{-\infty}^{0} \phi_x(0, y; t)\cos my \cdot dy, \quad (13)$$

in which $\tilde{\bar{\phi}}^{(p)}(s, m; t)$ is the Fourier cosine transform of $\bar{\phi}^{(p)}(s, y; t)$ and use has been made of the boundary conditions (11) and (12). Carrying out the integration on y by making use of (1), (4) and the boundary condition at $x = 0$ in (6) and by applying the first mean value theorem, $\tilde{\bar{\phi}}^{(p)}(s, m; t)$ is obtained in the form:

$$\tilde{\bar{\phi}}^{(p)}(s, m; t) = (2/\pi)q\,\frac{\cos md_0}{m^2 + s^2} \cdot \theta(t), \quad (14)$$

Applying the inverse transform in m, the following expression for $\bar{\phi}^{(p)}(s, y; t)$ is obtained:

$$\bar{\phi}^{(p)}(s, y; t) = (2/\pi)^{3/2}q\int_{-\infty}^{0} \frac{\cos md_0 \cdot \cos my \cdot dy}{m^2 + s^2}\,\theta(t). \quad (15)$$

The Fourier cosine transform in x is now applied to the free surface condition (5). By inserting (10) and (15) in the result, the equation determining the arbitrary function $A(s; t)$ is obtained in the form:

$$A_{tt}(s; t) + A_t(s; t) + gsA(s; t) = -(2/\pi)^{3/2}q\int_{-\infty}^{0} \frac{\cos md_0}{m^2 + s^2}\,dm\{\theta_{tt}(t) + \mu\theta_t(t)\}. \quad (16)$$

The initial conditions for $A(s; t)$ is derived from (7) by applying the Fourier cosine transform in x to (7) and by making use of (8), (10), and (15):

$$A(s; 0) = 0,\ A_t(s; 0) = -(2/\pi)^{3/2}q\dot{\theta}_0\int_{-\infty}^{0} \frac{\cos md_0}{m^2 + s^2}\,dm. \quad (17)$$

Applying the Laplace transform to (16), and applying the inverse transform based on the convolution theorem to the result, the arbitrary function $A(s; t)$ satisfying the initial condition (17) is obtained in the form:

$$A(s; t) = -(2/\pi)^{3/2}q\int_{-\infty}^{0} \frac{\cos md_0}{m^2 + s^2}\,dm \cdot \left[\theta(t) - \frac{gs}{\phi_0(s)}\int_0^t \theta(\tau)\exp\left\{-\frac{\mu}{2}(t - \tau)\right\}\sin\phi_0(s)(t - \tau)d\tau\right], \quad (18)$$

where the phase function $\phi_0(s)$ is given by

$$\phi_0(s) = \sqrt{gs - \mu^2/4}. \quad (19)$$

The expressions (15) and (18) are now inserted in (10), the inverse transform in s is applied to the result and the integration on s and m is carried out to obtain the following integral representation for the velocity potential $\phi(x, y; t)$:

$$\phi(x, y; t) = -\frac{2}{\pi}q\int_0^{\infty} \frac{e^{-sx}}{s}\sin d_0 s \cdot \sin ys \cdot ds \cdot \theta(t) + \frac{2}{\pi}qg\int_0^{\infty}\frac{(e^{(y-d_0)s}}{\phi_0(s)}\cos sx \cdot ds\int_0^t \theta(\tau)e^{-\frac{\mu}{2}(t-\tau)} \cdot \sin\phi_0(s)(t - \tau)d\tau, \quad (20)$$

Therefore, the transient hydrodynamical pressure $p(x, y; t)|_{x=0}$ exerted on the weir plate is given by the following integral representation:

$$p(x, y; t)|_{x=0} = -\rho\phi_t(x, y; t)|_{x=0} = \frac{2}{\pi}q\rho \cdot \lim_{x\to 0}\left[\int_0^{\infty}\frac{1}{s}e^{-sx}\sin d_0 s \cdot \sin ys \cdot ds \cdot \theta_t(t) - g\int_0^{\infty} e^{(y-d_0)s}\cos sx \cdot ds\int_0^t \theta(\tau)\,e^{-\frac{\mu}{2}(t-\tau)}\cos\phi_0(s)(t - \tau)d\tau\right], \quad (21)$$

where ρ is the specific mass of the fluid.

The Equation of Motion of the Tainter-Gate System. The transient hydrodynamical pressure $p(0, y; t)$ exerted on the weir plate turns the Tainter-gate about the Z-axis. Since the distance between the vector of the transient hydrodynamical pressure exerted on the weir plate and the Z-axis is assumed to be approximately constant R_*, the moment $M(t)$ which turns the Tainter-gate in the direction of the arrow shown in Fig. 2 is given by

$$M(t) = -c_gR_*\int_{-d_0}^{0} p(0, y; t)dy = -\frac{2}{\pi}q\rho c_g R_*\lim_{x\to 0}\int_{-d_0}^{0}\left[\int_0^{\infty}\frac{1}{s}e^{-sx}\sin d_0 s \cdot \sin ys \cdot ds \cdot \theta_t(t) - g\int_0^{\infty} e^{(y-d_0)s}\cos sx \cdot ds\int_0^t \theta(\tau)\,e^{-\frac{\mu}{2}(t-\tau)}\cos\phi_0(s)(t - \tau)d\tau\right] dy, \quad (22)$$

where it has been considered for the boundary values of the definite integral that both of the amplitude of surface waves and the change of the height of the discharge opening are very small compared with the depth d_0 of the discharge opening. R_* is defined as positive when the vector of the transient hydrodynamical pressure passes under the Z-axis and as negative when the vector passes over the Z-axis. c_g is a modification factor of area when the curved weir plate is replaced with a linear boundary.

The equation of motion to which the small oscillation of the Tainter-gate system from the equilibrium state is subject, is given by the following form:

$$\Theta_{tt}(t) + 2\omega_0\zeta\theta_t(t) + \omega_0^2\theta(t) = M(t)/I_0, \quad (23)$$

where ζ is the damping ratio and ω_0 the natural frequency as follows:

$$\zeta = \frac{\gamma_0}{2I_0\omega_0}, \quad \omega_0 = \sqrt{K_0R_b^2/I_0}. \quad (24)$$

On substitution of (22) into (23), the equation of motion of the Tainter-gate system is obtained as follows:

$$\theta_{tt}(t) + \left[2\omega_0\zeta + \frac{2}{\pi}\cdot\frac{q\rho c_g R_*}{I_0}\int_{-d_0}^{0} dy\int_0^{\infty}\frac{1}{s}\sin d_0 s \cdot \sin ys \cdot ds\right]\theta_t(t) + \omega_0^2\theta(t) = \frac{2}{\pi}\frac{q\rho c_g R_* g}{I_0}\lim_{x\to 0}\int_{-d_0}^{0} dy\int_0^{\infty} e^{(y-d_0)s}\cos sx \cdot ds\int_0^t \theta(\tau)e^{-\frac{\mu}{2}(t-\tau)}\cos\phi_0(s)(t - \tau) \cdot d\tau. \quad (25)$$

Since the integral term in the coefficient of $\theta_t(t)$ takes a negative value, the second term in the coefficient of $\theta_t(t)$ is always negative when R_* is positive. Therefore, it may be concluded from the above equation that the Tainter-gate system essentially possesses the primary factor of a self-excited oscillation. If the damping effects in the Tainter-gate system are very small, the coefficient of $\theta_t(t)$ takes a negative value. Therefore, when such a condition is at least satisfied, it seems that the Tainter-gate system easily grows up to a self-excited oscillatory one. However, since the terms of positive or negative damping are included also in the right-hand side of the above equation, more forcible discussions about this point cannot be made here. An exact analysis for the dynamical stability should be given.

The Dynamical Stability of the Tainter-Gate System

To analyze the dynamical stability of the Tainter-gate system which is subject to the equation of motion (25), the Nyquist stability theorem is applicable. The dimensions characteristic function $w'(p')$ of the equation of motion (25) is given by the following integral representation:

$$w'(p') = 1 + p'^2 + \left[2\zeta - \frac{k'}{\pi} \cdot \frac{R'd^2}{F'_0} \int_{-1}^{0} \left\{ -\frac{1}{2} \ln \frac{1+y'}{1+y'} + i\pi G(x)|_{x=0}\, e^{(y'-1)s'_0} + \int_0^\infty \frac{1}{s'^2 + s'^2_0} \left(s' \cos(1-y')s' - s'_0 \sin(1-y')s'\right) ds' \right\} dy' \right] p', \tag{26}$$

in which use has been made of the Kelvin's method of stationary phase [14, 15] to neglect the time dependent terms. $p'(= \xi'_p + \eta'_p)$ is the dimensionless complex variable and $y'(= y/d_0)$ the dimensionless water depth. The parameter R'_d, k' and F'_0 are given by

$$R'_d = d_0/R_a \sin \Theta_0, \quad k' = 2\sqrt{2} c_f c_0 \rho \, \frac{R_a^3 \cdot R_*}{I_0} \sin^2 \Theta_0 \cdot \cos \Theta_0,$$

$$F'_0 = \sqrt{d_0/g} \cdot \omega_0. \tag{27}$$

Since R'_d represents the ratio of the depth of the discharge opening to the height of the trunnion pin 0 from the discharge opening, it is called the dimensionless depth of the discharge opening. Since k' depends upon the moment of inertia, the shape and the size of the Tainter-gate, it is called the design factor of the Tainter-gate. F'_0 is the basic Froude number by which the flow pattern in the reservoir is determined fundamentally. The function $G(x)$ of the variable x is due to s'_0 which is given by

$$s'_0 = -F'^2_0(p'^2 + \mu' p') \tag{28}$$

When $\xi'_p = 0$, $G(x)|_{x=0}$ is given by

$$G(x)|_{x=0} = \left\{ \begin{array}{ll} -1 & \text{when } \xi'_p = 0, \eta'_p > 0, \\ 0 & \text{when } \xi'_p = 0, \eta'_p = 0, \\ +1 & \text{when } \xi'_p = 0, \eta'_p < 0. \end{array} \right\} \tag{29}$$

To analyze the stability of the Tainter-gate system by making use of the Nyquist stability criterion, the characteristic function $w'(p')$ from (26) is selected for a mapping function and the mapping from the p'-plane to the w'-plane is considered. The w'-plane is expressed as follows:

$$w'(p') = u'(\xi'_p, \eta'_p) + iv'(\xi'_p, \eta'_p), \tag{30}$$

When $\xi'_p = 0$ in the equation (26), the Nyquist functions $u'(0, \eta'_p)$ and $v'(0, \eta'_p)$ representing the Nyquist curve $w'(i\eta'_p)$ in the w'-plane are obtained in the following form:

$$u'(0, \eta'_p) = 1 - \eta_p'^2 + \eta'_p G(0) \, \frac{k'Rd'^2}{F'_0} \cdot u'_*(F_0),$$

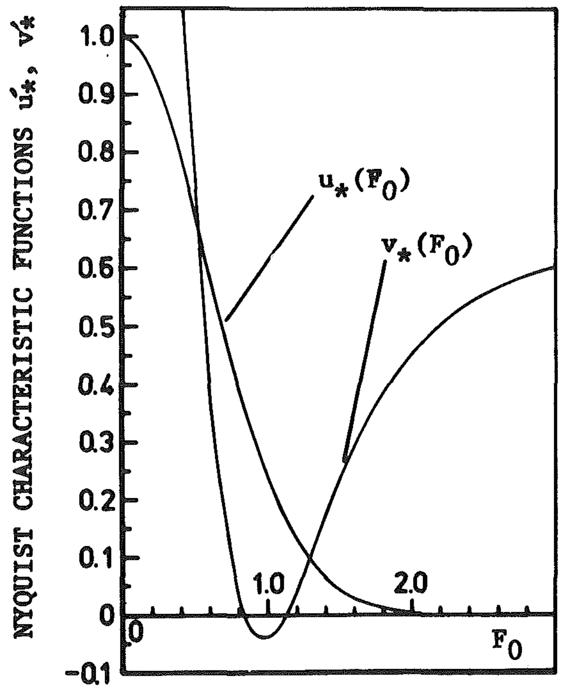

Fig. 4 Nyquist characteristic functions $u_*'(F_0)$, $v_*'(F_0)$

$$v'(0, \eta'_p) = \left[2\zeta - \frac{k'Rd'^2}{F'_0} \cdot v_*'(F_0)\right] \cdot \eta'_p, \tag{31}$$

where the functions $u_*'(F_0)$ and $v'_*(F_0)$ of the variable F_0 are given by

$$u'_*(F_0) = \frac{1}{F_0^2} \cdot \frac{1}{e^{F_0^2}} \left(1 - \frac{1}{e^{F_0^2}}\right),$$

$$v'_*(F_0) = \int_{-1}^{0} \left[-\frac{1}{2} \ln \frac{1+y'}{1-y'} + \int_0^\infty \frac{1}{s'^2 + F_0^4} \left\{ s' \cos(1-y')s' - F_0^2 \sin(1-y')s' \right\} ds' \right] \cdot dy', \tag{32}$$

where the variable F_0 is the general Froude number with the general frequency η_p and is defined as follows:

$$F_0 = F'_0 \cdot \eta'_p = \sqrt{d_0/g} \cdot \eta_p. \tag{33}$$

The small constant $\mu'(= \mu/\omega_0)$ representing the effect of small dissipative force in the fluid is replaced with zero in the equations (31) and (32). Since the functions $u'_*(F_0)$ and $v'_*(F_0)$ are the fundamental functions determining the characteristics of the Nyquist curve, these are called Nyquist characteristic functions. These functions are shown in Fig. 4, in which the abscissa is the general Froude number F_0.

Consider the contour Γ in the p'-plane, as shown in Fig. 5(a). It is easily known from (31) that the origin 0 of the p'-plane corresponds to the point 0' (1, i0) in the w'-plane. Considering the properties of the Nyquist characteristic functions, it is known that when the roving point p' in the p'-plane proceeds from (0, $-i\infty$) to (0, $+i\infty$) on the imaginary axis, the Nyquist curve $w'(i\eta'_p)$ for $k' > 0$ traces out the curve $\overrightarrow{(5'0'1')}$ shown in Fig. 5(b), and that for $k' < 0$ traces out the curve $\overrightarrow{(5'0'1')}$ shown in Fig. 5(c). When the roving point p' travels clockwise along the infinite semi-circular portion of Γ, the characteristic function $w'(p')$ for $k' > 0$ traces out the circle $\overrightarrow{(1'2'3'4'5')}$ shown in Fig. 5(b), and that for $k' < 0$ traces out the curve $\overrightarrow{(1'2'3'4'5')}$ shown in Fig. 5(c). The dotted portions of the lines shown in Fig. 5 correspond to negative values of η'_p, while the solid portions cor-

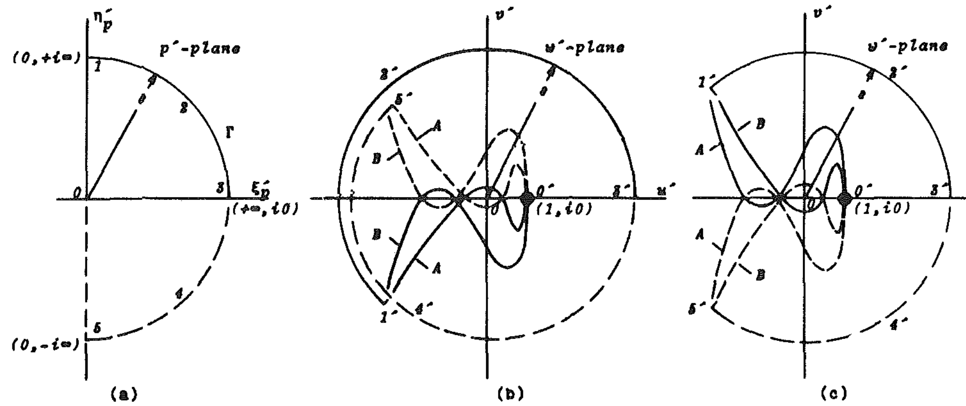

(a) The contour Γ (b) Nyquist plot for $k' > 0$ ($R_* > 0$) (c) Nyquist plot for $k' < 0$ ($R_* < 0$)

Fig. 5 Illustration showing the contour Γ in the p'-plane and its mapping in the w'-plane.

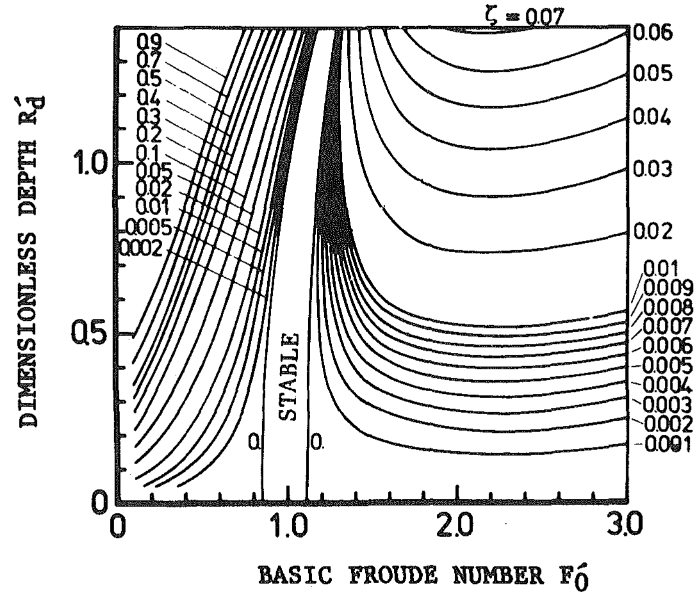

Fig. 6 Stability diagram of the Tainter-gate system for $k' = 1.0$

respond to positive values of η'_p. The plot in Figs. 5(*b*) and (*c*) illustrates a stable condition (A) and an unstable condition (B). For the curve B, the vector R makes two clockwise revolutions about the origin 0, whereas for the curve A it makes no net rotations. The difference between the curve A and B depends upon the dimensionless depth R'_d of the discharge opening, the basic Froude number F'_0, the design factor k' and the damping ratio ζ, which are contained in (31) as parameters. In this study, the stability diagram is expressed by R'_d as ordinate, F'_0 as abscissa and k' and ζ as parameters.

For the design factor $k' > 0$, i.e. $R_* > 0$: The stability diagram for $k' = 1.0$ is shown in Fig. 6. This stability diagram shows the values of R'_d and F'_0 which yield stable, unstable and periodic solutions of the equation (25). If the point (R'_d, F'_0) lies in the lower region of the curves, bounded solutions of (25) are obtained. If the point (R'_d, F'_0) lies in the upper region of the curves, the solutions are unbounded. If the point (R'_d, F'_0) lies on the curves, the solutions are periodic. When $\zeta = 0$, the stable region is restricted within the narrow region in the neighborhood of $F'_0 = 1.0$. The unstable region is wide. As ζ increases, however, the stable region grows wide. The rate that the stable region grows wide for $F'_0 > 1.0$ is far larger than for $F'_0 < 1.0$. When ζ is larger than about 0.07, there exists no unstable region in $F'_0 > 1.0$, whereas the considerably wide region of unstable remains in $F'_0 < 1.0$, even if ζ has a fairly large value. In order to examine the influence that the design factor exerts the stability of the Tainter-gate system, the stability diagram for $\zeta = 0.03$ is shown in Fig. 7. It is known in this figure that as k' increases, the stable region becomes narrow rapidly, whereas the unstable region extends toward the region of small R'_d. For example, the stability diagram for $k' = 5.0$ is as shown in Fig. 8.

For the design factor $k' < 0$, i.e. $R_* < 0$: The stability diagram for $k' = -1.0$ is shown in Fig. 9. On the contrary to the previous case, the stable region is far wide. As ζ increases, the stable region becomes more wide. When ζ is larger than about 0.02, there exists no unstable region in Fig. 9. As $|k'|$ increases, however, the unstable region becomes wide, as seen from the stability diagram for $\zeta = 0.003$ shown in Fig. 10. This property is the same as that for $k' > 0$. The stability diagram for $k' = -5.0$ is as shown in Fig. 11. There exists some unstable region, even if ζ has fairly large value.

Model Experiments for the Stability of the Tainter-Gate System

In order to confirm the theoretically obtained characteristics of self-excited oscillation, the following model for the Tainter-gate system and the reservoir was made: The model used for experiments is shown in Fig. 12. The Tainter-gate system is situated at the left-hand side. The size of the reservoir is 1500 mm long, 500 mm high and 40 mm wide. Since water is supplied from a circulation system, the water level of the reservoir is able

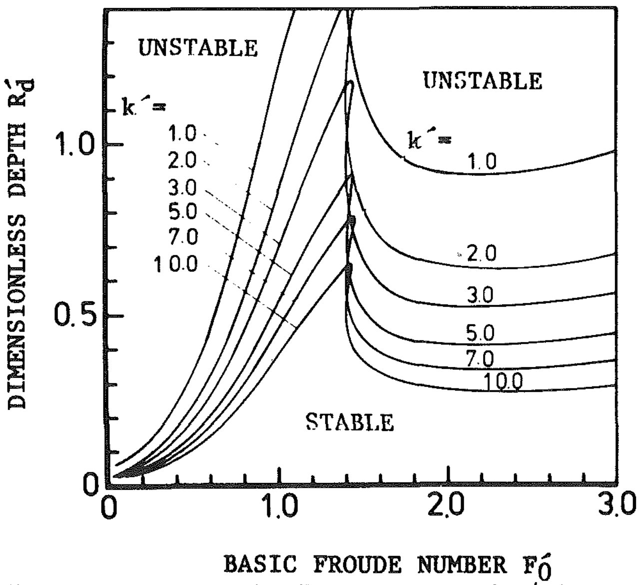

Fig. 7 Stability diagram of the Tainter-gate system for $k' > 0$, $\zeta = 0.03$

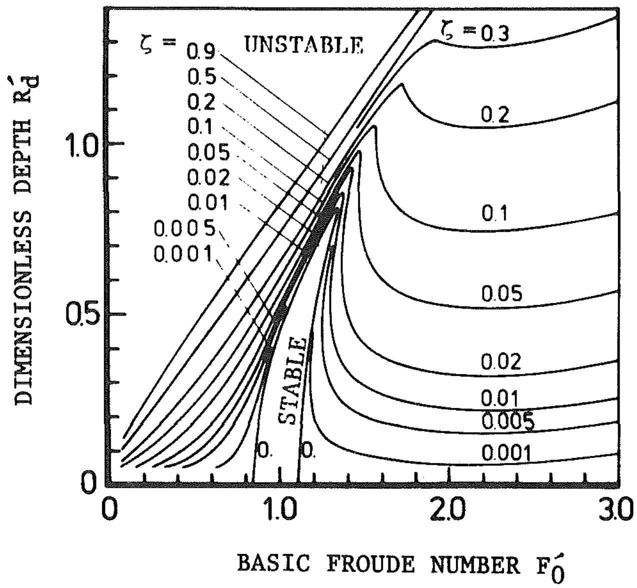

Fig. 8 Stability diagram for the Tainter-gate system for $k' = 5.0$

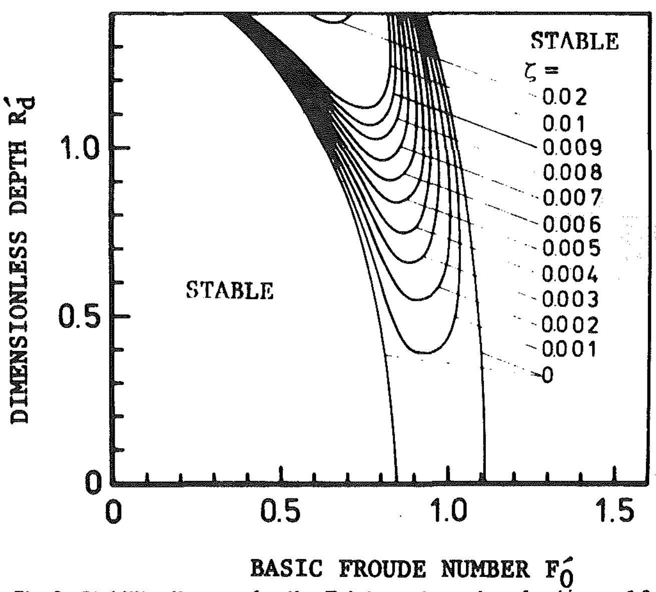

Fig. 9 Stability diagram for the Tainter-gate system for $k' = -1.0$

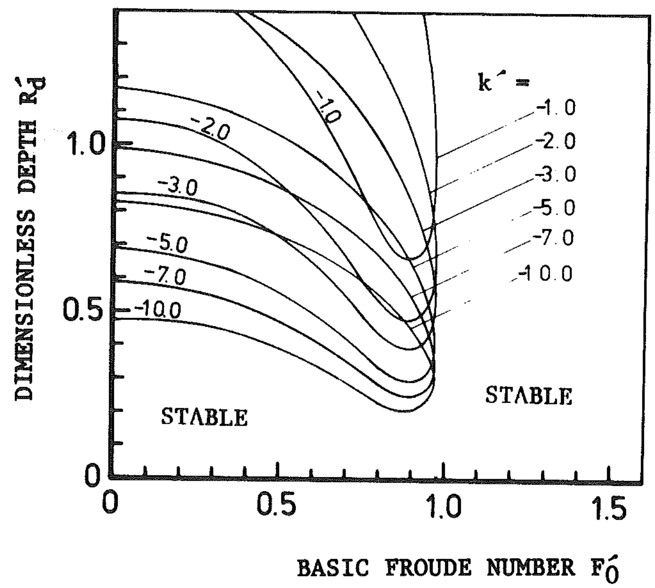

Fig. 10 Stability diagram of the Tainter-gate system for $k' < 0$, $\zeta = 0.003$

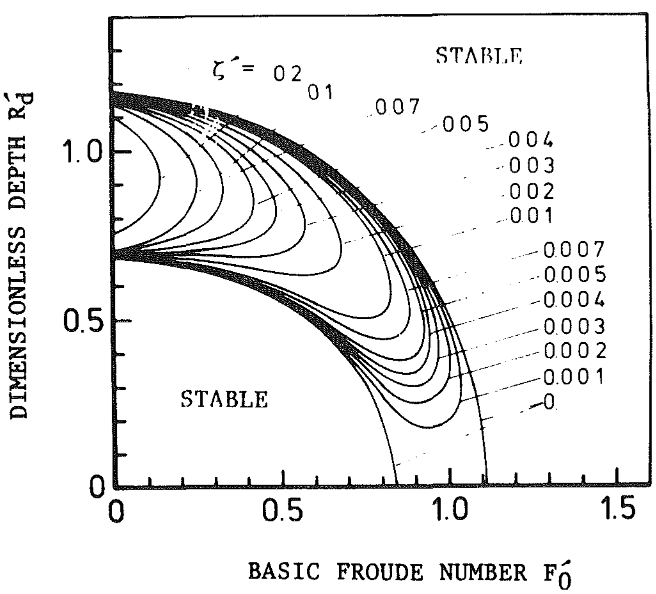

Fig. 11 Stability diagram of the Tainter-gate system for $k' = -5.0$

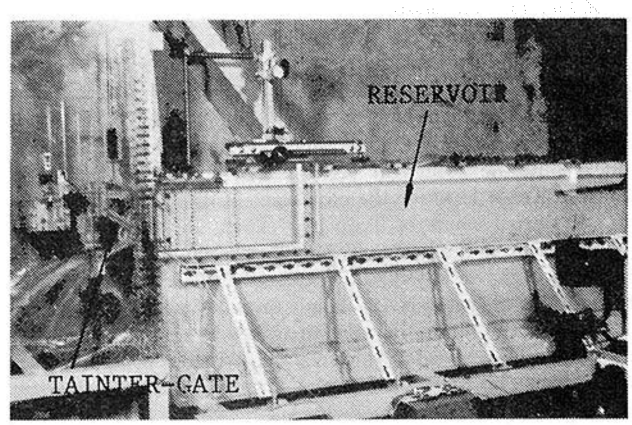

Fig. 12 A model for the Tainter-gate system and the reservoir

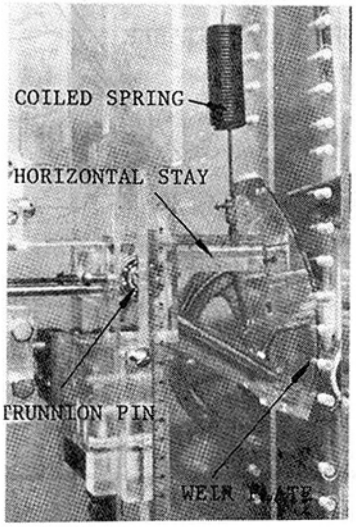

(*a*) **The model of the Tainter-gate system**

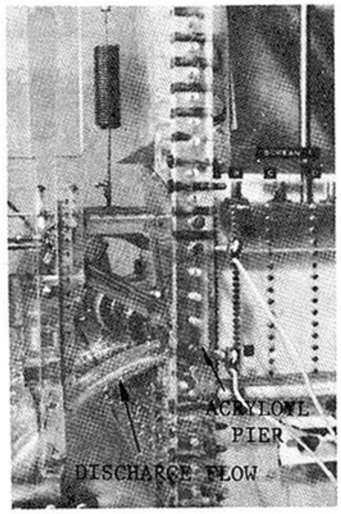

(*b*) **The Tainter-gate system under a steady discharge**

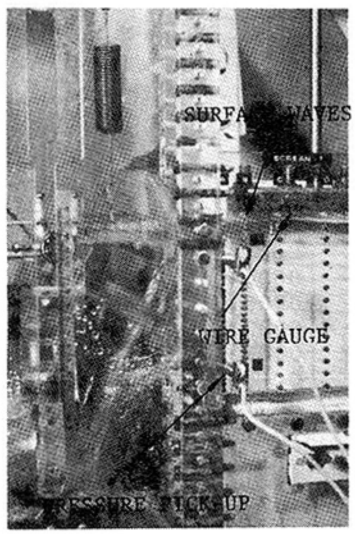

(*c*) **The Tainter-gate system under being self-excited and the surface waves induced on the reservoir surface**

Fig. 13 A model for the Tainter-gate system

to be kept constant. The height of the discharge opening from the bottom of the reservoir is 330 mm and that of the trunnion pin is 422 mm. The model of the Tainter-gate system is shown in (*a*) of Fig. 13. The center of the weir plate with a radius of 135 mm is situated under the trunnion pin. As the position of support of a coiled spring is able to be traversed, the natural frequency of the model is adjustable. The vertical position of its support is also adjustable, to set the upper stay of the model always horizontally. The dimensions, the modification factor of area c_g and the coefficient of discharge c_f for the model are shown in Table 1, where the coefficient of discharge was quoted from the experiments of Toch [6]. Then, the design factor k' for the model is 1.19. The Tainter-gate system under a steady discharge is shown in (*b*) of Fig 13. As the vertical position of the model is adjustable, the height b of the discharge opening was set down to 5 mm, in order to satisfy the assumption in the theory that the steady discharge quantity is comparateively small. The weir plate has a width of 40 mm and the clearance between the sidewall of the weir plate and the acryloylpier was set down to about 0.02 mm. The Tainter-gate system being self-excited and the surface waves induced on the back water are shown in (*c*) of Fig. 13. Surface waves are measured with a handmade resistance wire gage, the transient hydrodynamical pressure with a pressure pick-up vertically attached to the wall of the reservoir and the behavior of the Tainter-gate with a displacement pickup which is noncontacting.

Table 1 The dimensions, the modification factor of area and the coefficient of discharge for the model

R_a (cm)	R_b (cm)	R_* (cm)	Θ_0 (deg)	I_0 $\left(\frac{g \cdot cm \cdot s^2}{cm}\right)$	c_g	c_f
13.8	11.7	3.01	39.2	2.72	1.04	0.6

Examples of the experimental records for the model are shown in Fig. 14. An example for $(R'_d, F'_0) = (1.88, 1.66)$, i.e. the stable Tainter-gate system is shown in (*a*) of Fig. 14. The motion stops entirely in about 2 seconds after an initial disturbance. As is to be expected from the previous study [8], the surface

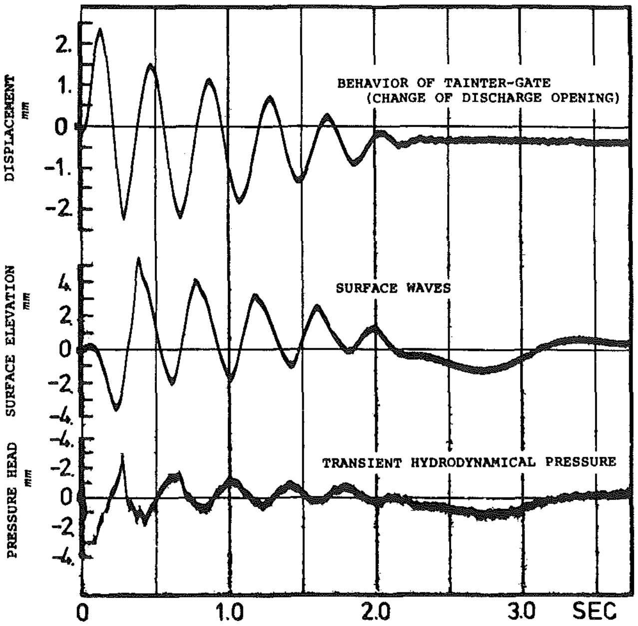

Fig. 14(a) An experimental record for the stable Tainter-gate system: $(R_d', F_0') = (1.88 \pm 0.03, 1.66 \pm 0.05)$, the positive damping ratio 0.060 ± 0.005

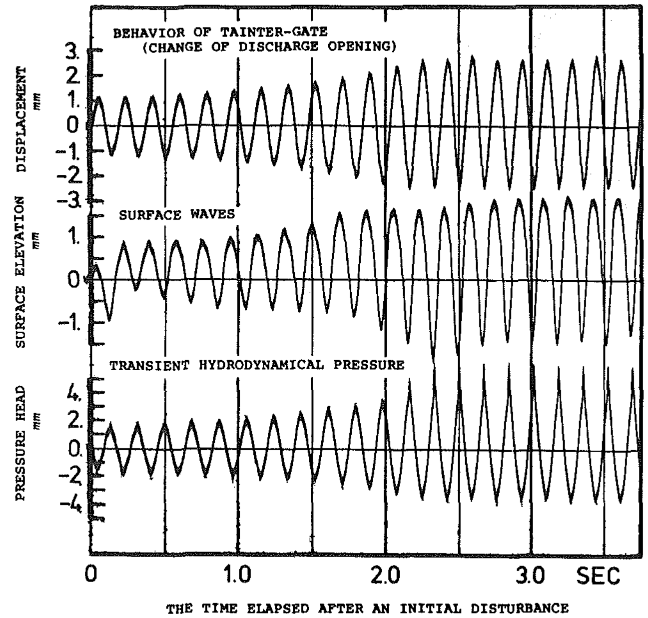

Fig. 14(b) An experimental record for the unstable Tainter-gate system: $(R_d', F_0') = (1.88 \pm 0.03, 3.52 \pm 0.05)$, the negative damping ratio -0.013 ± 0.007

Fig. 14 Experimental records for the stable and the unstable Tainter-gate system. The measured position of surface waves: $(x', y') = (0.16 \pm 0.01, 0)$, that of transient hydrodynamical pressure: $(x', y') = (0.15 \pm 0.01, -0.74 \pm 0.03)$

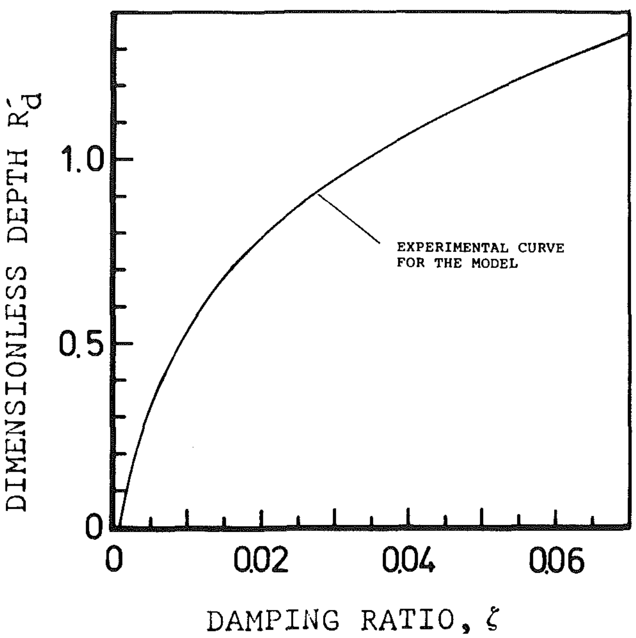

Fig. 15 The experimentally evaluated characteristics of the damping ratio in the model for the Tainter-gate system (the uncertainity band for R_d' is $\pm$ 0.03, that for $\zeta \pm 0.003$)

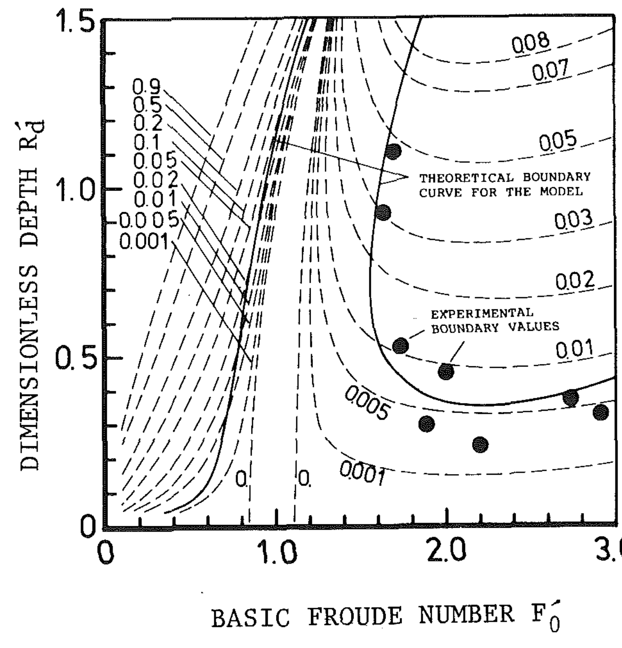

Fig. 16 Boundary values of the stable and the unstable region for the model of the Tainter-gate system which design factor $k' = 1.19 \pm 0.05$ (the uncertainty band for R_d' is $\pm$ 0.03, that for $F_0' \pm 0.05$, that for the damping ratio $\pm$ 0.003)

waves with comparatively large amplitudes are induced. The kinetic energy of the gate itself is being rapidly absorbed in the waves. An example for $(R'_d, F'_0) = (1.88, 3.52)$, i.e. the unstable Tainter-gate system is shown in (*b*) of Fig. 14. The Tainter-gate system is growing up to a self-excited oscillatory system, with the negative damping ratio -0.013. The growth is completed in about 2 seconds after an initial disturbance and the lower edge of the weir plate begins to collide with acryloyly pier. The strains in the pressure wave are caused by this fact. The surface waves induced on the headwater have comparatively small amplitudes. Therefore, the energy that the fluid supplies to the Tainter-gate becomes larger than that absorbed in the surface waves.

As the dimensionless depth R'_d of the discharge opening increases, the mass added of the fluid and the hydraulic friction exerted on the gate become larger. Therefore, the damping ratio ζ in the system becomes larger, as R'_d increases. In order to compare the experimental results with the theoretical ones, the relation of R'_d and ζ must be previously obtained. Fig. 15 shows its relation which was experimentally obtained, based on the following simple consideration: When the Tainter-gate under a boundary state of the stable and the unstable region is periodically oscillating, all of the energies that the fluid supplies to the Tainter-gate are absorbed in the damper. Therefore, the experimentally obtained damping ratio ζ represents all of the damping effects in the system. The solid portions of the lines in Fig. 16 show the theoretical boundary curves for stability corresponding to this characteristics for the damping ratio. The dotted portions show the theoretical boundary curves for the constant damping ratios. The signs (•) show the experimentally obtained boundary values for stability. Since the size of the reservoir used for the experiments was not so large, the natural frequency of the water in the reservoir was comparatively high. For this reason, the experimental values for the theoretical boundary curve in the lower region of F'_0 could not be obtained. The theoretical boundary curve in higher region of F'_0, however, is in good agreement with the experimental results. Hence, the assumptions in the theoretical analysis for the Tainter-gate system should be considered to be reasonable.

Conclusions

It is considered that Tainter-gates are the most reliable type of crest gate for passage of large floods. If the fundamental principle of the gate that the weir plate is made concentric to the trunnion pin is satisfied, Tainter-gates may be surely the most reliable. However, if this fundamental principle is not satisfied, one is no longer able to expect that Tainter-gates are the most reliable. To lighten the hoisting load of the gate, Tainter-gates are often designed so that the center of the weir gate is situated over the trunnion pin. On the contrary, to raise the static stability of Tainter-gates, they are sometimes designed so that the center of the weir plate is situated under the trunnion pin. Furthermore, even if Tainter-gates are designed so that the weir plate is concentric to the trunnion pin, they are not always made as designed.

This study made clear that Tainter-gates possess unstable characteristics, provided that the center of the weir plate is not in agreement with the trunnion pin. Such dynamical characteristics for Tainter-gates were confirmed with experiments. The characteristics for the stability are as follows: Though an economical design in structural strength tends to be made with no fear in designing Tainter-gates, it makes the design factor $|k'|$ large. As the rate $|R_*|$ that the center of the weir plate is not in agreement with the trunnion pin increases, the deisgn factor $|k'|$ becomes larger. Therefore, these primary factors fostor the dynamical instability of Tainter-gates. The stability for $R_* > 0$ and $R_* < 0$ is different as follows: When $R_* > 0$, i.e. the center of the weir plate is situated under the trunnion pin, the static stability is raised. However, there exists a considerably wide region of instability, and Tainter-gates fall into a very dangerous state. It is impossible to entirely avoid such an instability, even if there exists a large damping effect in the Tainter-gate system. When $R_* < 0$, i.e. the center of the weir plate is situated over the trunnion pin, the hoisting load of the gate becomes light. Tainter-gates, however, are unstable in some restricted region. This instability is entirely avoidable, provided that the natural frequency of the system and the depth of discharge opening is so large that the basic Froude number F'_0 is larger than about 1.1. Especially when the design factor $|k'|$ is comparatively small, the existence of a moderate damping effect mades Tainter-gates unconditionally stable. When the design factor $|k'|$ is comparatively large, however, there exists some unstable region for the small F'_0, even if the damping effect is comparatively large.

In designing Tainter-gates, the fundamental design that the weir plate is made concentric to the trunnion pin is the best. This fundamental policy for design should be exactly kept. However, the careful considerations for the dynamical characteristics of Tainter-gates make a design for lightening the hoisting load possible. It should be absolutely avoided to design Tainter-gates so that the center of the weir plate is situated under the trunnion pin. It is very dangerous to make an economical design in structural strength of Tainter-gates, with no fear.

References

1 Ishii, N., "Instability of Elastically Suspended Tainter-Gate System Caused by Surface Waves on the Reservoir of Dam," The Dissertation presented to Osaka University, at Toyonaka, Osaka, Japan 560, in Mar. 1975.

2 Linsley, R. K., and Frazini, J. B., *Water Resources Engineer*, McGraw-Hill, 1972, p. 245.

3 Davis, C. V., and Sorensen, K. E., *Handbook of Applied Hydraulics*, McGraw-Hill, 1969, pp. 21–1.

4 *ASAHI EVENING NEWS*, July 3, 1967.
ASAHI NEWSPAPER, July 3 and 26, 1967 (in Japanese).

5 Chow, Ven Te, *Open-Channel Hydraulics*, McGraw-Hill, 1959, p. 507.

6 Toch, A., "Discharge Characteristics of Tainter-gates," *Transactions, American Society of Civil Engineers*, Vol. 120, 1955, pp. 290–300.

7 Larock, B. E., "Gravity-Affected Flow from Planar Sluice Gate," *Journal of the Hydraulic Division, Proceedings of the American Society of Civil Engineers*, Vol. 95, No. HY4, 1969.

8 Ishii, N., and Imaichi, K., "Water Waves and Structural Loads Caused by a Periodic Change of Discharge from a Sluice-Gate," *Bulletin of the Japan Society of Mechanical Engineers*, Vol. 20, No. 146, Aug. 1977.

9 Imaichi, K., and Ishii, N., "Instability of an Idealized Tainter-Gate System Without Damping Caused by Surface Waves on the Backwater of Dam," *Bulletin of the Japan Society of Mechanical Engineers*, Vol. 20, No. 146, Aug. 1977.

10 Rayleigh, J. W. S., *The Theory of Sound*, Dover Publication, 1945.

11 Rayleigh, J. W. S., "The Form of Standing Waves on the Surface of Running Water," *Proceedings of London Mathematical Society*, 15–69, 1883, p. 1883.

12 Lamb, H., *Hydrodynamics*, Cambridge University Press, 1932.

13 Lamb, H., "On Deep-Water Waves," *Proceedings of London Mathematical Society*, Series 2, 2–388, 1904.

14 Stoker, J. J., *Water Waves*, Interscience Publication, Inc., New York, 1957, p. 163.

15 Baker, B. B., and Compson, E. T., *The Mathematical Theory of Huygens' Principle*, The Clarendon Press, Oxford, 1939.